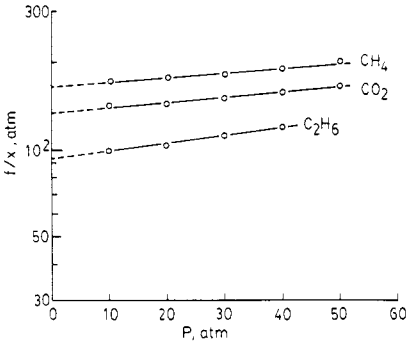

Figure 6. Plot of ln (f/x) vs. p at 300 °C.

ture and pressure. The multiple solubility data are generally reproducible to within 1.5% in mole fraction of the dissolved solute. Individual measurements are shown in Figures 1–3 as separate points where they can be distinguished. The observed gas solubilities increase with increasing pressure and decreasing temperature.

In Figure 3 we include the carbon dioxide solubility data of Gasem and Robinson (*1*) at 100 °C for comparison. The agreement of their data and ours seems reasonable with our data being a shade lower, the largest difference amounting to 2.5%.

Henry's constant and partial molar volume at infinite dilution are determined from the solubility data by plotting ln (f/x) of the solute at a temperature as a function of pressure. The fugacity f is calculated for the pure solute gas by using the Lee–Kesler correlation (*3*). Figures 4–6 show the linear result that is obtained. By the equation of Krichevsky and Kasarnovsky (*4*), the intercept at pressure (p) equal to the vapor pressure of the solvent determines Henry's constant, and the slope gives the partial molar volume at infinite dilution. Table II presents the results. The Henry's constant values are estimated to be uncertain to about 3%; the partial molar volume values to about 10%. Figure 7 shows Henry's constant as a function of temperature. Our results agree well with those of Gasem and Robinson for CO_2 mixtures.

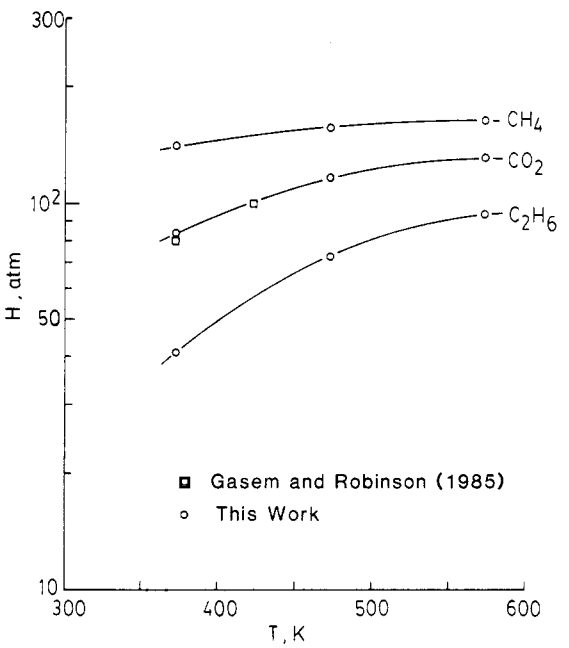

Figure 7. Henry's constant of methane, ethane, and carbon dioxide in *n*-hexatriacontane.

Registry No. CO_2, 124-38-9; CH_4, 74-82-8; C_2H_6, 74-84-0; hexatriacontane, 630-06-8.

Literature Cited

(1) Gasem, K. A. M.; Robinson, R. L., Jr., *J. Chem. Eng. Data* **1985**, *30*, 53.
(2) Huang, S. H.; Lin, H. M.; Chao, K. C. *Fluid Phase Equilib.*, in press.
(3) Lee, B. I.; Kesler, M. G. *AIChE J.* **1975**, *21*, 510.
(4) Krichevsky, I. R.; Kasarnovsky, J. S. *J. Am. Chem. Soc.* **1935**, *57*, 2168.

Received for review January 28, 1987. Accepted June 19, 1987. This work was supported by the Department of Energy through Contract DE-AC22-84PC70024.

High-Pressure Specific Heat Capacities of Pure Water and Seawater

Chen-Tung A. Chen

Institute of Marine Geology, Sun Yat-Sen University, Kaohsiung, Taiwan, 80424, Republic of China

Equations of state for pure water and seawater were used to calculate high-pressure specific heat capacities at constant pressure (C_p) and at constant volume (C_v). Equations are given for pure water C_p and C_v values over the temperature range of 0–100 °C and pressure range of 0–1000 bar. Equations are also given for seawater C_p and C_v values over the salinity range of 0–40, temperature range of 0–40 °C, and pressure range of 0–1000 bar. These equations agree with the direct measurements reported in the literature for pure water to within ±0.026% over the measurement ranges of 20–100 °C up to 500 bar. No direct-pressure seawater measurements are available for comparison.

Introduction

Among the thermodynamic properties of pure water and seawater, the specific heat capacity is of primary importance. For instance, if two water masses of differing salinity and temperature are mixed uniformly, the resultant temperature and density are a function of heat capacity. Also, heat capacity data are needed for estimating the heat storage capacity of the oceans, for converting sound speeds to isothermal compressibilities, and for computing the adiabatic temperature gradient and static stability of waters. The data are also used in the investigation of structural changes of water.

Several pure water and seawater heat capacity measurements have been made at 1 atm (*1–6*). Because of experimental difficulties, however, no direct measurement has yet

0021-9568/87/1732-0469$01.50/0

Table I. Check Values of Specific Heat Capacities ($J\ g^{-1}\ K^{-1}$) at Various Salinities, Temperatures, and Pressures

t, °C	p, bar	C_p	C_v
	$S = 0$		
0	0	4.2188	4.2163
0	1000	3.9117	3.8809
100	0	4.2140	3.7668
100	1000	4.0329	3.6300
	$S = 35$		
0	0	3.9879	3.9862
0	1000	3.7629	3.7127
25	0	3.9981	3.9372
25	1000	3.8309	3.7173

been made at elevated pressures for seawater; only one set of data for pure water exists, and only for pressures below 500 bar (*7*). The available high-pressure data (*8–11*, *13*) were generated from the following equations

$$C_p^P = C_p^0 - T\int_0^P \partial^2 V/\partial T^2\, dP \quad (1)$$

$$C_v = C_p + T(\partial V/\partial T)^2/((\partial V/\partial P) \quad (2)$$

where C_p and C_v are respectively the heat capacity under constant pressure and the heat capacity under constant volume; superscripts P and 0 denote absolute pressures P and 0 (1 atm), respectively, T is the absolute temperature, and V is the specific volume of seawater.

Since the 1 atm pure water measurements of Osborne et al. (*6*), based on IPTS-48, form the basis of most heat capacity measurements, proper conversion of their data to the IPTS-68 scale must be made (*12*). We used the IPTS-68 scale in our study.

Specific Heat Capacity

Since many of the relevant seawater thermodynamic properties used in this study were measured relative to pure water (*5*, *13–17*), specific heat capacities for pure water were generated first. The 1 atm C_p values were taken directly from Kell (*12*).

$$C_{p,w}^0 = 4.21875 - 3.70271 \times 10^{-3}t + 1.382704 \times 10^{-4}t^2 - 2.860003 \times 10^{-6}t^3 + 3.523475 \times 10^{-8}t^4 - 2.30539 \times 10^{-10}t^5 + 6.247 \times 10^{-13}t^6 \quad (3)$$

The sound-derived pure water equation of state Chen et al. (*15*) was then combined with eq 1 and 3 to generate C_p^P over the temperature range of 0–100 °C and pressure range of 0–1000 bar. The results were fit to a polynomial function of temperature and pressure with a precision of ±0.0003 $J\ g^{-1}\ K^{-1}$.

$$C_{p,w}^P\ (J\ g^{-1}\ K^{-1}) = C_{p,w}^0 + A_{p,w}P + B_{p,w}P^2 + C_{p,w}P^3 \quad (4)$$

$$A_{p,w} = -4.9504 \times 10^{-4} + 1.3831 \times 10^{-5}t - 3.0118 \times 10^{-7}t^2 + 3.5717 \times 10^{-9}t^3 - 2.1623 \times 10^{-11}t^4 + 4.790 \times 10^{-14}t^5 \quad (5)$$

$$B_{p,w} = 2.4296 \times 10^{-7} - 8.2085 \times 10^{-9}t + 1.4083 \times 10^{-10}t^2 - 1.1969 \times 10^{-12}t^3 + 4.407 \times 10^{-15}t^4 \quad (6)$$

$$C_{p,w} = -5.493 \times 10^{-11} + 1.512 \times 10^{-12}t - 1.162 \times 10^{-14}t^2 \quad (7)$$

Values generated from eq 3–7 at selected temperatures and pressures are plotted in Figure 1. Check values are given in Table I.

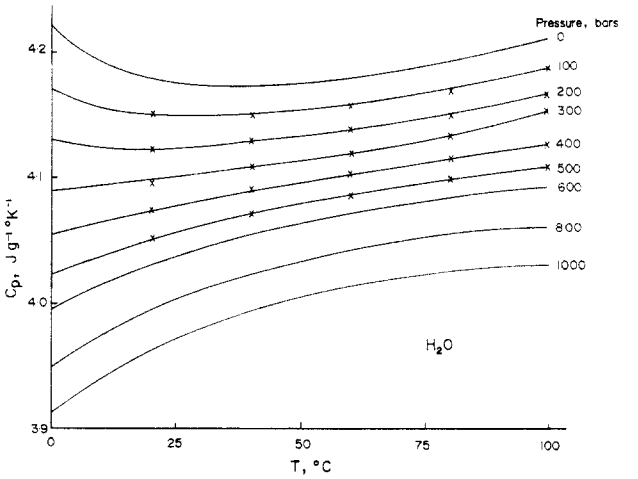

Figure 1. Pure water C_p data obtained from this study (smooth lines) and from Sirota and Shrago (crosses).

The specific heat capacities under constant volume, C_v, can be calculated with the use of eq 2. The values calculated from C_p and eq 2 over the range of 0–100 °C and 0–1000 bar were fit to the following equations with a standard deviation of ±0.000 15 $J\ g^{-1}\ K^{-1}$.

$$C_{v,w}^P\ (J\ g^{-1}\ K^{-1}) = C_{v,w}^0 + A_{v,w}P + B_{v,w}P^2 + C_{v,w}P^3 \quad (8)$$

$$C_{v,w}^0 = 4.21628 - 2.3956 \times 10^{-3}t - 3.934 \times 10^{-5}t^2 + 3.291 \times 10^{-7}t^3 - 3.845 \times 10^{-9}t^4 + 3.724 \times 10^{-11}t^5 - 1.335 \times 10^{-13}t^6 \quad (9)$$

$$A_{v,w} = -4.6812 \times 10^{-4} + 6.666 \times 10^{-6}t - 6.282 \times 10^{-8}t^2 + 2.174 \times 10^{-10}t^3 + 2.467 \times 10^{-12}t^4 - 1.902 \times 10^{-14}t^5 \quad (10)$$

$$B_{v,w} = 1.6744 \times 10^{-7} - 3.733 \times 10^{-9}t + 3.479 \times 10^{-11}t^2 - 1.202 \times 10^{-13}t^3 \quad (11)$$

$$C_{v,w} = -3.473 \times 10^{-11} + 8.348 \times 10^{-13}t - 5.15 \times 10^{-15}t^2 \quad (12)$$

Values generated from eq 8–12 at selected temperatures and pressures are plotted in Figure 2a. Check values are given in Table I.

The 1 atm seawater values needed to generate C_p^P values were taken from the equation of Millero et al. (*5*).

$$C_{p,s}^0 = C_{p,w}^0 + (-7.644 \times 10^{-3} + 1.073 \times 10^{-4}t - 1.3839 \times 10^{-6}t^2)S + (1.77 \times 10^{-4} - 4.08 \times 10^{-6}t + 5.35 \times 10^{-8}t^2)S^{1.5} \quad (13)$$

The seawater C_p^P values over the salinity range of 0–40, temperature range of 0–40 °C and pressure range of 0–1000 bar were then generated from the seawater equation of state of Chen and Millero (*17*) and eq 1 and 13. Chen and Millero's equation of state was chosen because it is more precise than other equations (*18*, *19*) deduced from a larger data base.

The C_p values were fit to the following equations with a standard deviation of ±0.0011 $J\ g^{-1}\ K^{-1}$.

$$C_{p,s}^P\ (J\ g^{-1}\ K^{-1}) = C_{p,s}^0 + A_{p,s}P + B_{p,s}P^2 + C_{p,s}P^3 \quad (14)$$

$$A_{p,s} = A_{p,w} + (3.8643 \times 10^{-6} - 4.048 \times 10^{-8}t - 5.305 \times 10^{-10}t^2 + 1.697 \times 10^{-11}t^3)S + (1.707 \times 10^{-9} - 5.748 \times 10^{-9}t)S^{1.5} \quad (15)$$

$$B_{p,s} = B_{p,w} + (-1.952 \times 10^{-9} + 2.679 \times 10^{-11}t)S \quad (16)$$

$$C_{p,s} = C_{p,w} + 4.231 \times 10^{-13}S \quad (17)$$

Values of C_p^P for seawater at 35 salinity are plotted in Figure 2b at various temperatures and pressures. Check values are given in Table I.

Values of C_v^P were calculated from the C_p^P values and eq 2. They were then fit to the following equation with a standard deviation of ±0.0011 J g^{-1} K^{-1}.

$$C_{v,s}^P \text{ (J g}^{-1}\text{ K}^{-1}) = C_{v,s}^0 + A_{v,s}P + B_{v,s}P^2 + C_{v,s}P^3 \quad (18)$$

$$C_{v,s}^0 = C_{v,w}^0 + (-7.2607 \times 10^{-3} + 1.2486 \times 10^{-5}t + 1.8974 \times 10^{-6}t^2 - 3.1412 \times 10^{-8}t^3)S + (1.1606 \times 10^{-4} + 2.3382 \times 10^{-6}t - 1.572 \times 10^{-7}t^2 + 1.401 \times 10^{-9}t^3)S^{1.5} \quad (19)$$

$$A_{v,s} = A_{v,w} + (2.4186 \times 10^{-6} + 4.8723 \times 10^{-8}t - 2.590 \times 10^{-9}t^2 + 3.709 \times 10^{-11}t^3)S + (5.1726 \times 10^{-8} - 7.1627 \times 10^{-9}t)S^{1.5} \quad (20)$$

$$B_{v,s} = B_{v,w} + (-1.2783 \times 10^{-9} + 9.893 \times 10^{-12}t)S \quad (21)$$

$$C_{v,s} = C_{v,w} + 3.228 \times 10^{-13}S \quad (22)$$

Values of C_v^P for seawater at 35 salinity are plotted in Figure 2c at various temperatures and pressures. Check values are given in Table I.

Discussion and Conclusion

Sirota and Shrago (*7*) published the only high-pressure pure water heat capacity data (C_p) obtained from direct measurements. Their data, plotted in Figure 1, agree with our results to within ±0.026% (1σ). Since Sirota and Shrago reported their data to 0.1%, the agreement may be considered excellent.

Figure 1 indicates that pure water C_p decreases with increasing temperature at low temperatures and pressures, but increases with increasing temperatures at higher temperatures and pressures. C_p decreases with pressure over the entire temperature range studied. The rate of decrease ($\partial C_p/\partial P$) decreases rapidly with pressure (Figure 3a).

Figure 2a shows that pure water C_v decreases monotonically with pressure and temperature over the ranges studied. The rate of C_v decrease with pressure ($\partial C_v/\partial P$) also decreases with pressure, but at a slower rate than $\partial C_p/\partial P$ (Figure 3a). No direct high-pressure C_v data are available for comparison with our data.

Figure 2b shows the variation of C_p with temperature and pressure for seawater with a salinity of 35. C_p agrees very well with the derived values of Fofonoff (*10*) and Fofonoff and Millard (*11*) at pressures below 600 bar. Our values, however, are lower at higher pressures, especially at 40 °C. Other C_p values reported in the literature (*9*, *13*) were derived from less accurate equations of state and are probably not very accurate.

C_p data shown in Figure 2b behave like pure water C_p values at high pressures (above 600 bar) and increase monotonically with temperature. In other words, dissolved sea salts in a seawater with a salinity of 35 induce an internal pressure of approximately 600 bar. The salinity dependence on C_p is plotted vs. salinity in Figure 3b. The absolute $\partial C_p/\partial S$ values decreases with increasing salinity.

Figure 2c shows the temperature and pressure dependence of C_v of seawater at a salinity of 35. Pressure decreases C_v over the temperature range studied. At low pressures, C_v values decrease monotonically with temperature. At higher pressures, however, C_v values increase with temperature initially, go through a maximum, and then decrease with temperature at higher temperatures. Sea salts also depress C_v (Figure 3b), significantly, similar to what was found for C_p. No high-pressure C_v measurements have been reported for seawater.

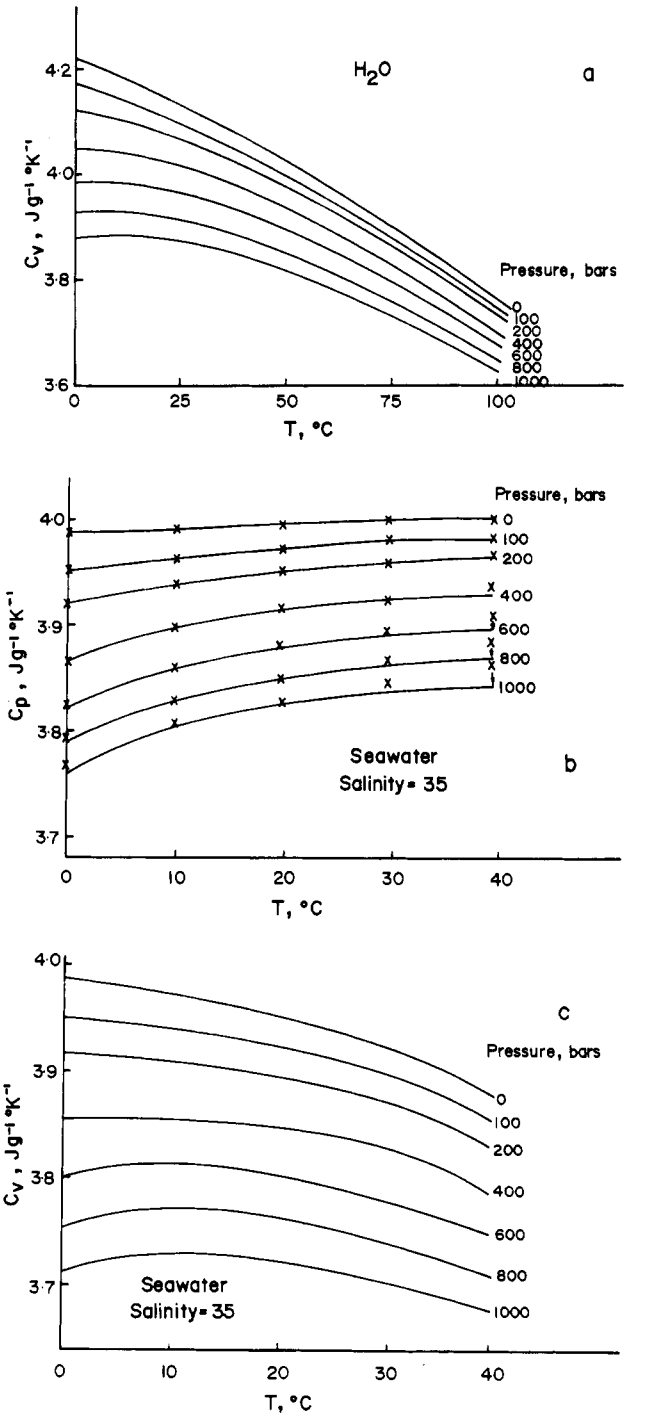

Figure 2. (a) Pure water C_v, and (b) C_p and (c) C_v of seawater at 35 salinity vs. temperature and pressure. Crosses in (b) denote data from ref *10* and *11*.

In summary, equations of state for pure water and seawater were used to calculate high-pressure specific heat capacities at constant pressure (C_p) and at constant volume (C_v). Equations are given for pure water C_p and C_v values over the temperature range of 0–100 °C and pressure range of 0–1000 bar. Equations are also given for seawater C_p and C_v values over the salinity range of 0–40, temperature range of 0–40 °C, and pressure range of 0–1000 bar. These equations agree with the direct measurements reported in the literature for pure water

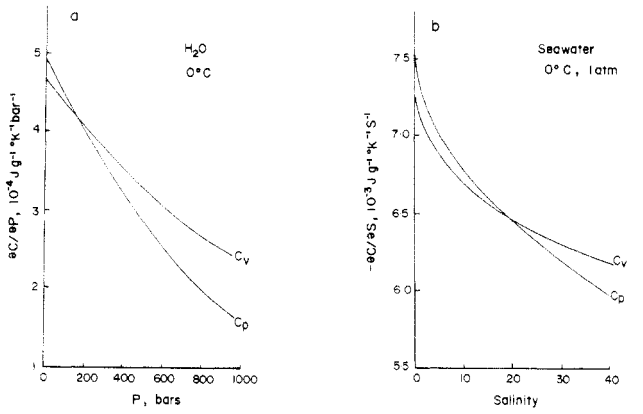

Figure 3. Plots of (a) $\partial C_p/\partial P$ and $\partial C_v/\partial P$ for pure water at 0 °C, and (b) $\partial C_p/\partial S$ and $\partial C_v/\partial S$ vs. salinity for seawater at 0 °C and 1 atm.

to within ±0.026% over the measurement ranges of 20–100 °C and up to 500 bar.

Glossary

C_p	specific heat capacity at constant pressure, J g^{-1} K^{-1}
C_v	specific heat capacity at constant volume, J g^{-1} K^{-1}
J	joules
P	absolute pressure
T	absolute temperature, K
t	temperature, °C
V	specific volume

Registry No. H_2O, 7732-18-5.

Literature Cited

(1) Bromley, L. A. *J. Chem. Eng. Data* **1968**, *13*, 60–62.
(2) Bromley, L. A.; Desaussure, V. A.; Clipp, J. C.; Wright, J. S. *J. Chem. Eng. Data* **1967**, *12*, 202–205.
(3) Bromley, L. A.; Diamond, A. E.; Salami, E.; Wilkins, D. G. *J. Chem. Eng. Data* **1970**, *15*, 246–253.
(4) Cox, R. A.; Smith, N. D. *Proc. R. Soc. London* **1959**, *A252*, 51–62.
(5) Millero, F. J.; Perron, G.; Desnoyers, J. E. *J. Geophys. Res.* **1973**, *78*, 4499–4507.
(6) Osborne, N. S.; Stimson, H. F.; Ginnings, D. C. *J. Res. Natl. Bur. Stand.* **1939**, *23*, 197.
(7) Sirota, A. M.; Shrago, Z. Kh. *Teploenergetika* **1968**, *15*, 86–90.
(8) Chen, C. T. *J. Chem. Eng. Data* **1982**, *27*, 356–358.
(9) Fofonoff, N. P. *The Sea*; Hill, M. N., Ed.; Interscience: New York, 1962; Vol. 1, pp 3–30.
(10) Fofonoff, N. P. *J. Geophys. Res.* **1985**, *90*, 3332–3342.
(11) Fofonoff, N. P.; Millard, R. C. Jr. *UNESCO Tech. Pap. Mar. Sci.* **1983**, *44*, 53.
(12) Kell, G. S., unpublished, 1977; Division of Chemistry, National Research Council Canada, Ottawa, Canada.
(13) Chen, C. T. M.S. Thesis, University of Miami 1974, p 258.
(14) Chen, C. T.; Millero, F. J. *Deep-Sea Res.* **1976**, *23*, 595–612; **1977**, *24*, 265–269.
(15) Chen, C. T.; Fine, R. A.; Millero, F. J. *J. Chem. Phys.* **1977**, *66*, 2142–2144.
(16) Chen, C. T.; Fine, R. A.; Millero, F. J. *Deep-Sea Res.* **1978**, *25*, 499–501.
(17) Chen, C. T.; Millero, F. J. *J. Mar. Res.* **1978**, *36*, 657–691.
(18) Millero, F. J.; Chen, C. T.; Bradshaw, A.; Schleicher, K. *Deep-Sea Res.* **1980**, *27A*, 255–264.
(19) Millero, F. J.; Chen, C. T.; Bradshaw, A.; Schleicher, K. *UNESCO Tech. Pap. Mar. Sci.* **1981**, *38*, 99–188.

Received for review September 15, 1986. Accepted May 26, 1987. This work was partially supported by the National Science Council of the Republic of China (NSC 76-0209-M110-03).

Solubility of Nonpolar Gases in Halogenated Compounds. 1. Solubility of H_2, D_2, N_2, O_2, CH_4, C_2H_4, C_2H_6, CF_4, SF_6, and CO_2 in Chlorocyclohexane at 263.15–303.15 K and 101.32 kPa of Partial Pressure of Gas

María C. López, María A. Gallardo, José S. Urieta, and Celso Gutiérrez Losa*

Departamento de Química Física, Facultad de Ciencias, Ciudad Universitaria, 50009, Zaragoza, Spain

Solubility measurements of several nonpolar gases (H_2, D_2, N_2, O_2, CH_4, C_2H_4, C_2H_6, CF_4, SF_6, and CO_2) in chlorocyclohexane have been determined from 263.15 to 303.15 K at a partial pressure of gas of 101.32 kPa. Experimental results are compared with those obtained from Hildebrand's semiempirical approach. Partial molal Gibbs energy, partial molal enthalpy, and partial molal entropies of solution at 298.15 K and 101.32 kPa of partial pressure of gas are evaluated.

Introduction

As is well-known, gas solubility in liquids plays an important role both from the theoretical and the practical point of view. In fact, it is a suitable base for studying liquid structure and for characterizing molecular interactions.

This paper is a part of a more extensive study of solubility of nonpolar gases in halogenated derivatives of benzene and cyclohexane. We report here solubility measurements of several nonpolar gases (H_2, D_2, N_2, O_2, CH_4, C_2H_4, C_2H_6, CF_4, SF_6, and CO_2) in chlorocyclohexane between 263.15 and 303.15 K, at a partial pressure of gas of 101.32 kPa. Similar experimental measurements on other systems, together with a more detailed discussion of them, will be presented in subsequent papers.

Experimental Section

The solubility apparatus, similar to that used by Ben Naim and Baer (*1*) was housed in a thermostat within ±0.1 K. Its detailed